Direct Measurements of the Luzon Undercurrent

DUNXIN HU,* SHIJIAN HU,+ LIXIN WU,# LEI LI,# LINLIN ZHANG,* XINYUAN DIAO,@ ZHAOHUI CHEN,# YUANLONG LI,+ FAN WANG,* AND DONGLIANG YUAN*

* *Institute of Oceanology, Chinese Academy of Sciences, and Key Laboratory of Ocean Circulation and Wave, Chinese Academy of Sciences, Qingdao, China*
+ *Institute of Oceanology, Chinese Academy of Sciences, and Key Laboratory of Ocean Circulation and Wave, Chinese Academy of Sciences, Qingdao, and University of Chinese Academy of Sciences, Beijing, China*
# *Physical Oceanography Laboratory, Ocean University of China, Qingdao, China*
@ *Institute of Oceanology, Chinese Academy of Sciences, and R&D Center of Marine Environmental Engineering and Technology, Chinese Academy of Sciences, Qingdao, China*

(Manuscript received 5 September 2012, in final form 23 January 2013)

ABSTRACT

The Luzon Undercurrent (LUC) was discovered about 20 years ago by geostrophic calculation from conductivity–temperature–depth (CTD) data. But it was not directly measured until 2010. From November 2010 to July 2011, the LUC was first directly measured by acoustic Doppler current profiler (ADCP) from a subsurface mooring at 18.0°N, 122.7°E to the east of Luzon Island. A number of new features of the LUC were identified from the measurements of the current. Its depth covers a range from 400 m to deeper than 700 m. The observed maximum velocity of the LUC, centered at about 650 m, could exceed 27.5 cm s^{-1}, four times stronger than the one derived from previous geostrophic calculation with hydrographic data. According to the time series available, the seasonality of the LUC strength is in winter > summer > spring. Significant intraseasonal variability (ISV; 70–80 days) of the LUC is exposed. Evidence exists to suggest that a large portion of the intraseasonal variability in the LUC is related to the westward propagation of mesoscale eddies from the east of the mooring site.

1. Introduction

A southward flow under the Kuroshio to the east of Luzon Island was found by Hu and Cui (1989, 1991) from an inversion manipulation with conductivity–temperature–depth (CTD) data from three fall cruises in 1986, 1987, and 1988. They claimed that the flow was below 500 m with a maximum velocity of 6–7 cm s^{-1} and a transport of about 2 Sv (1 Sv $\equiv 10^6\ m^3\ s^{-1}$). This flow was later named the Luzon Undercurrent (LUC) by Qu et al. (1997), who used hydrographic data from 14 cruises in either fall or spring from 1986 to 1991, confirmed the existence of the southward-flowing LUC, and claimed its maximum speed of 7 cm s^{-1} at about 700 m and mean geostrophic volume transport of 3.6 Sv. In the last 15 years, studies on the LUC were focused on its characteristics or origin (e.g., Qu et al. 1998, 1999; Xie et al. 2009; Gao et al. 2012; Wang and Hu 2012).

Currents in the upper 500-m layer along the 18°20′N section were directly measured by a shipborne ADCP in December 2006 and January 2008 (Kashino et al. 2009) though the records are too shallow to capture the LUC. As a matter of fact, there was no direct current measurement of the LUC in previous studies until a subsurface current mooring equipped with an ADCP was deployed at about 18.0°N, 122.7°E in November 2010 and recovered in July 2011 from research vessel *Science 1*. The deployment of this subsurface mooring is a part of the field experiment of the Northwestern Pacific Ocean Circulation and Climate Experiment (NPOCE), which was endorsed by Climate Variability and Predictability (CLIVAR)/World Climate Research Programme (WCRP) in 2010 as an international joint program. NPOCE is designed to observe, simulate, and understand the dynamics of the northwestern Pacific Ocean circulation and its roles in the climate system (for details please see http://npoce.qdio.ac.cn). In the area to the east of Luzon, the

Corresponding author address: Dunxin Hu, Institute of Oceanology, Chinese Academy of Sciences, 7 Nanhai Road, Qingdao 266071, China.
E-mail: dxhu@qdio.ac.cn

DOI: 10.1175/JPO-D-12-0165.1

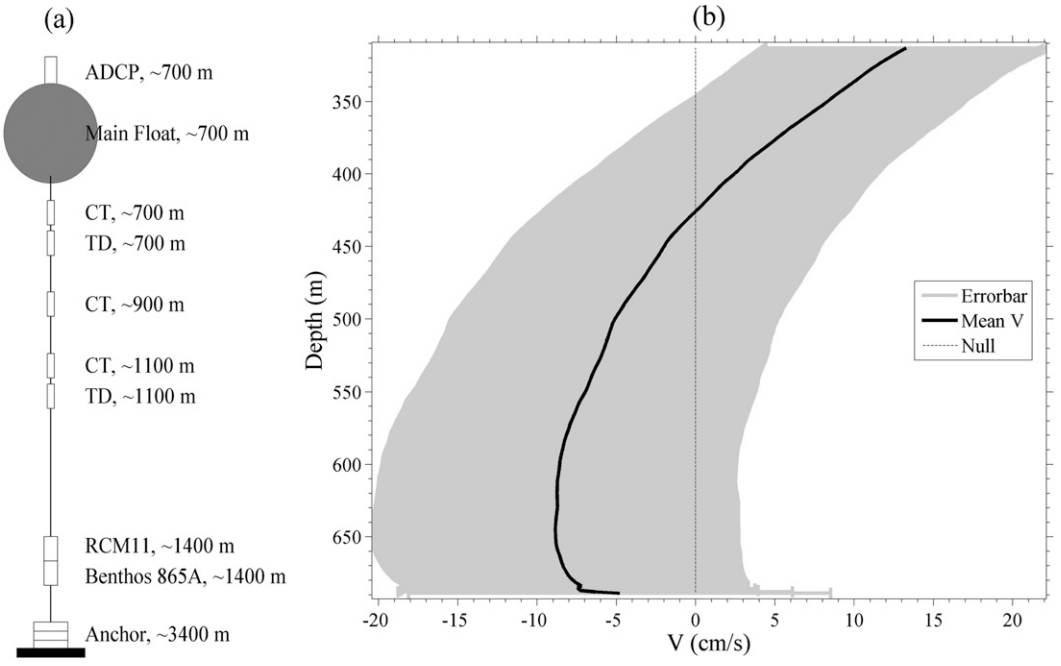

FIG. 1. (a) Simplified schematic diagram (nonproportional) of the configuration of the subsurface mooring buoy. (b) Time mean of 11-day running mean meridional component of velocity (i.e., *V*; black line) with std dev (gray) during the observation stage at the station 18.0°N, 122.7°E.

other observations carried out have implemented CTDs, lowered ADCPs, Argo floats, and so forth. In addition to the above, observations using subsurface moorings and other measurements were also conducted to the east of Mindanao Island by the NPOCE program. Based on the current data from the mooring to the east of Luzon Island, some new features of the LUC are ferreted out and presented in the present paper.

2. Data and methods

a. ADCP data processing

The data collected from the subsurface mooring at about 18.0°N, 122.7°E are applied in this study. A schematic diagram (nonproportional) of the mooring configuration is depicted in Fig. 1a. The mooring was equipped with an upward-looking 75-KHz Teledyne RD Instruments (TRDI) acoustic Doppler current profiler (ADCP), while an ALEC conductivity–temperature (CT) and an ALEC COMPACT temperature–depth (TD) were placed 12 m below the ADCP. Above the acoustic release (Benthos 865A), a Recording Current Meter 11 (RCM11) was attached at 1400-m depth.

The in situ temperature and salinity data measured by CT and TD are applied to calculate the in situ sound speed and bin length and then correct the original ADCP velocity data (Urick 1983; Kutsuwada and Inaba 1995; TRDI document ''Long Ranger Data Analysis''). The ADCP measured velocity every 30 min in 60 bins at depths ranging from about 200 to 700 m during the entire period. The successive values including velocity and depth were first averaged to build up hourly data for each layer, and then the velocity data were interpolated vertically at standard depths of 1-m vertical resolution. Finally, hourly velocity data at standard depths were subsampled to construct daily data. In this paper, these daily data are used to investigate the currents at the mooring site. It can be told from the orientation data of ADCP that the mooring line was tight and tensed enough during the whole observation period and the errors caused by pressure linear interpolation could be minor enough to be negligible. As the depth of ADCP was quite stable except for a few days from 27 to 30 April 2011, the errors induced by the up–down motion of the buoy were not taken into consideration.

b. Satellite data and HYCOM assimilation

The Delayed Time (DT) Updated (Upd) merged weekly gridded sea level and corresponding surface geostrophic current data from December 2010 to July 2011 are produced by the Data Unification and Altimeter Combination System (DUACS) and distributed by Archiving, Validation, and Interpretation of Satellite Data in Oceanography (AVISO)/Centre National d'Études Spatiales (http://www.aviso.oceanobs.com/duacs/, viewed on 2 May 2012).

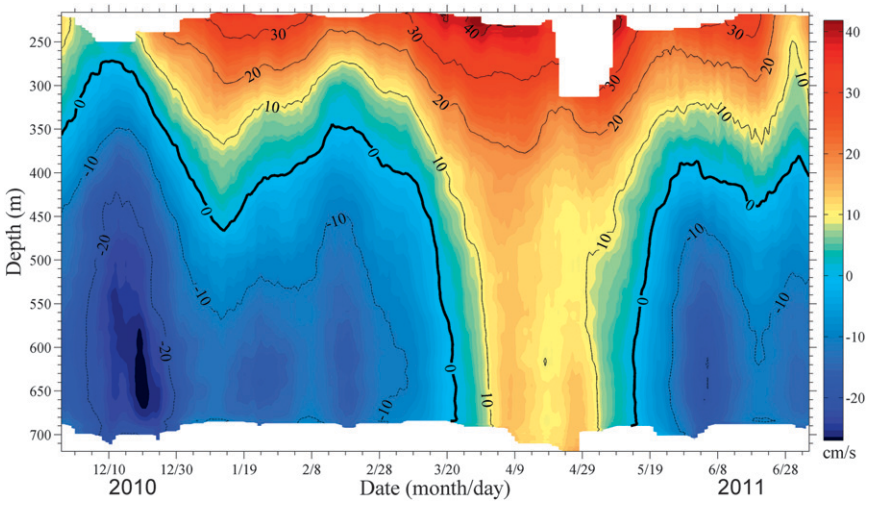

FIG. 2. Daily meridional current as a function of depth and time in mooring data. Tidal effect is excluded with an 11-day running mean. The contour interval is 10 cm s^{-1}. Negative values denote southward currents and positive values indicate northward currents.

The eddy-resolving Hybrid Coordinate Ocean Model (HYCOM) assimilation from Naval Research Laboratory (NRL) is used to examine the role of the mesoscale eddies around the mooring site in the variability of the LUC. They are daily data with variable horizontal (6.5-km grid spacing on average, 3.5-km grid spacing at the North Pole), and vertical (32 hybrid layers including 0, 10, 20, 30, 50, 75, 100, 125, 150, 200, 250, 300, 400, 500, 600, and 700 m in the upper 700 m) meshes. Observations including SSH [*Envisat*, *Geosat* Follow-On (GFO), and *Jason-1*], all available satellite and in situ SST, all available in situ temperature and salinity profiles (e.g., Argo floats, CTDs, moorings), and Special Sensor Microwave Imager (SSMI) sea ice concentration are assimilated with the three-dimensional multivariate optimum interpolation Navy Coupled Ocean Data Assimilation (NCODA) system (Chassignet et al. 2009). The quality of the HYCOM assimilation is examined in section 3c(2).

3. Results

a. Features of LUC exposed

The time-averaged meridional velocities V in each layer are shown in Fig. 1b. Between 424 and 689 m, the currents are southward with a maximum speed of about 9 cm s^{-1} around 645 m, corresponding to the core of LUC.

To remove the tidal effect, a central 11-day running mean is applied to the daily velocity data because main

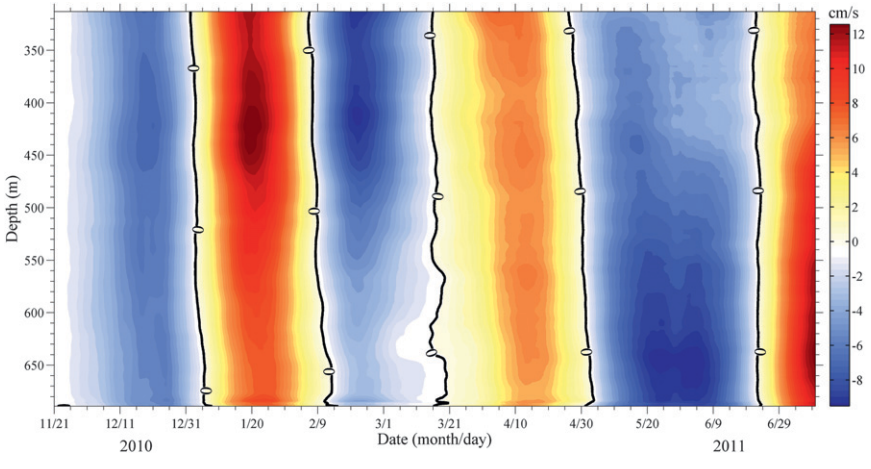

FIG. 3. Depth–time plot of 20–90-day bandpass-filtered time series of the meridional current anomaly.

TABLE 1. Vertical phase speeds of ISV (i.e., w_{ISV}), westward-propagating speed U, and eddy-induced vertical phase speed w_{eddy} in each segment.

	Segment number						
	1	2	3a	3b	4	5a	5b
w_{ISV} (m day^{-1})	88	88	349	−88	50	27	−70
U (cm s^{-1})	5	9	7	7	11	9	7
w_{eddy} (m day^{-1})	87	148	220	113	43	67	58

tidal periods here are found to be shorter than 10 days, and the resultant currents are shown in Fig. 2. The currents above about 300 m are northward, which should be part of the Kuroshio. From about 400 to 700 m, the currents are southward, representing the LUC. However, the currents are northward at all depths from 21 March to 15 May 2011. So far it is still unknown whether this is caused by a shift of the LUC route from the mooring spot or by other sudden events in the subsurface, which we do not know yet. During the whole observation period from boreal winter to midsummer, the maximum speed of the southward currents could exceed 27.5 cm s^{-1} near the core of LUC at about 650 m, which is about four times stronger than 6–7 cm s^{-1} geostrophically calculated by Hu and Cui (1989, 1991) and Qu et al. (1997). At the same time, the maximum of the northward flow below about 200 m, which should be a part of the Kuroshio, is approximately 43.1 cm s^{-1} at about 225 m during the whole period. As there are no observations above 200 m, the core of the Kuroshio cannot be determined with the obtained data available.

In addition, the strongest LUC takes place in the boreal winter (December) at 450–700 m, while the weakest in the boreal spring (around April, Fig. 2). Thus, from the observed time series available, the LUC seasonality seems to be that LUC (winter) > LUC (summer) > LUC (spring), which is in accordance with the result of a previous study using geostrophic calculation (Qu and Lukas 2003).

b. *Intraseasonal variability*

As shown in Fig. 2, there are 5 LUC cores during the whole period of the observation, which suggests a significant intraseasonal variability (ISV) of the LUC. To demonstrate the ISV of the LUC, a 20–90-day bandpass filter is applied to the daily meridional current anomalies relative to the mean over the whole period. A striking feature in V_{ISV} (intraseasonal filtered series) is the regular "bands" (Fig. 3), indicating significant ISV with a period from approximately 70 to 80 days (about 6 "bands", i.e., 3 cycles in 233 days). To simplify the discussion, we define seven segments 1, 2, 3a, 3b, 4, 5a, and 5b as the ISV of the observation periods between 21 November 2010 and 5 January 2011, 6 January 2011 and 8 February 2011, 9 February 2011 and 19 February 2011,

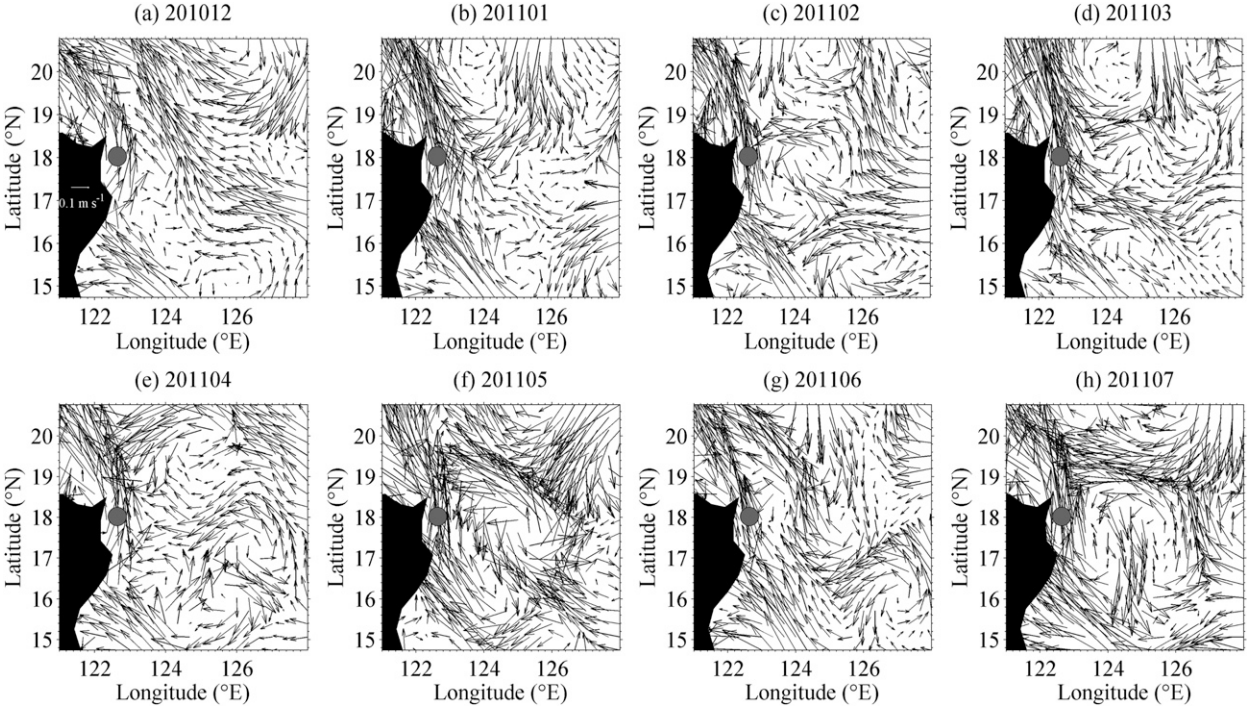

FIG. 4. (a)–(h) Monthly-mean surface geotropic currents anomaly around the mooring site from December 2010 to July 2011 based on satellite data. The gray dot denotes the mooring. A reference vector is provided in (a).

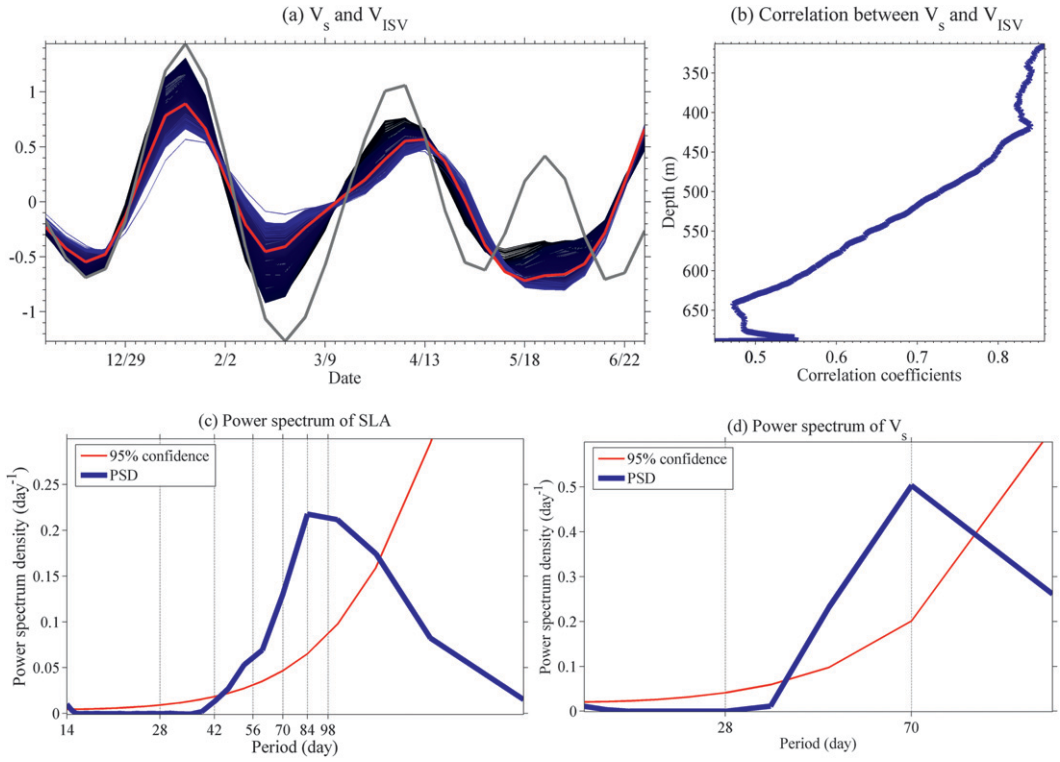

FIG. 5. (a)–(d) Comparison of satellite data (SLA and V_s) with ADCP measurements (V_{ISV}). (a) Thin lines from black to blue are V_{ISV} at depths from 313 to 689 m with 1-m interval, while thick red and gray lines denote 450-m V_{ISV} and V_s.

20 February 2011 and 20 March 2011, 21 March 2011 and 30 April 2011, 1 May 2011 and 30 May 2011, and May 31 2011 and 24 June 2011, respectively.

Another striking feature in Fig. 3 is the nearly parallel slope of the ''bands'' vertically and it seems that the ISV phase propagates downward in segments 1, 2, 3a, 4 and 5a, but upward in segments 3b and 5b. The ISV vertical-propagating speed w_{ISV} between two depths can be roughly estimated by calculating the lead-lag time between them for each segment. As shown in Fig. 3, w_{ISV} (vertical phase speed of ISV) at different depths are quite different. For this reason, we estimate w_{ISV} every 50 m vertically and then calculate the vertical-mean w_{ISV} of each segment (see Table 1). The mechanism of the vertical propagation (both downward and upward) of the ISV phase will be discussed in the following section.

c. *What causes the ISV of the LUC?*

Previous studies show that the mesoscale eddy can affect the mean flow significantly, including subsurface currents (e.g., Roemmich and Gilson 2001; Qiu and Chen 2010; Zhao and Luo 2010; Zheng et al. 2011). In addition, subthermocline eddies were found and could cause the intraseasonal variability of the subsurface currents off Mindanao Island (Firing et al. 2005; Dutrieux 2009; Qu et al. 2012). Thus, both surface and subthermocline eddies could play essential roles in the formation of the LUC ISV.

1) RESULTS BASED ON OBSERVATIONS

It is indicated by surface geostrophic current anomalies from satellite data that mesoscale eddies are energetic to the east of the mooring (Fig. 4). They switch between cyclonic and anticyclonic eddies alternatively and last for 2–3 months. The normalized areal-mean (17.62°–18.26°N, 122.33°–123.00°E) sea level anomaly (SLA) and surface meridional current anomaly (V_s) from satellite data are compared with the ADCP measured velocities (V_{ISV}) at different depths. SLA and V_s are 3–13-week bandpass filtered, and V_{ISV} is 20–90-day bandpass filtered. Power spectrum of SLA (Fig. 5c) and that of V_s (Fig. 5d) both show sharp peaks of about 70–90 days, which agrees well with the dominant period of the observed subsurface currents. That indicates mesoscale eddies to the east of Luzon Island going intraseasonally. It can be found through comparing Fig. 3 with Fig. 4 that a strong cyclonic eddy in December 2010 corresponds to a weaker Kuroshio and stronger LUC, while an anticyclonic eddy in March–May 2011 corresponds to a stronger Kuroshio and weaker LUC. The

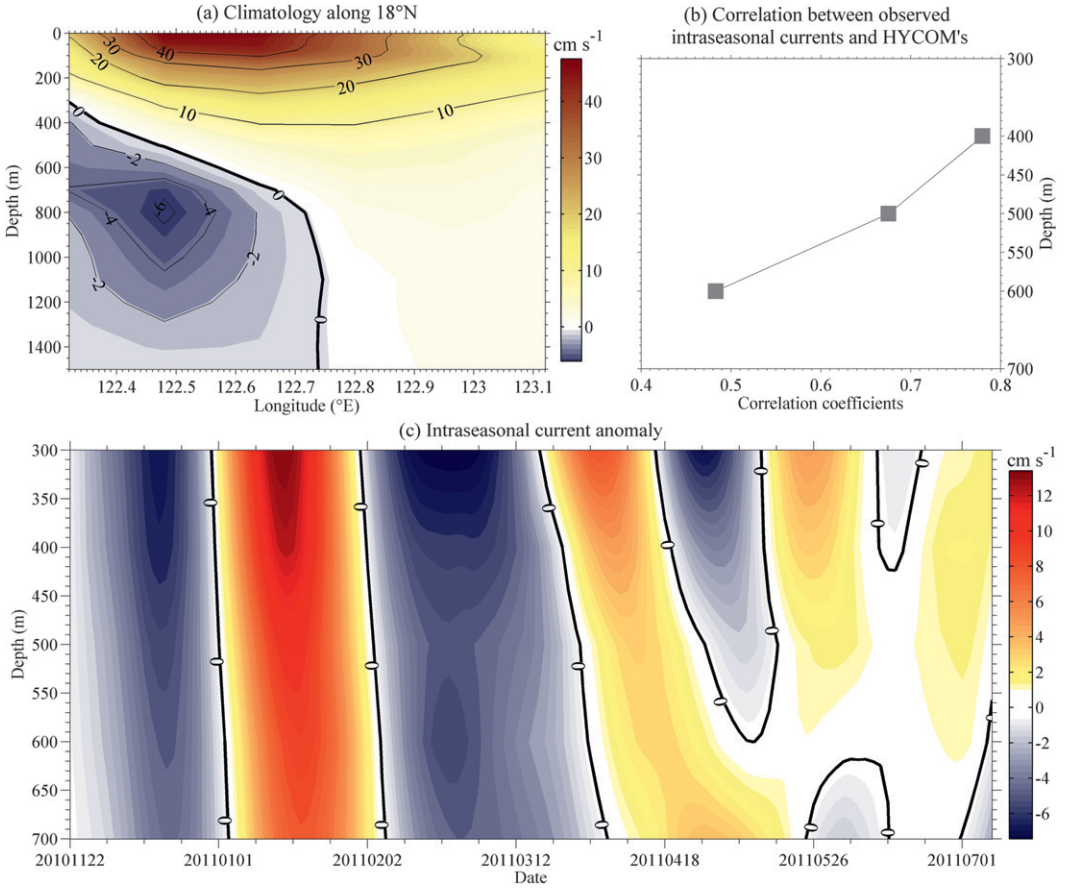

FIG. 6. Quality inspection of HYCOM assimilation from the perspective of the LUC. (a) The climatological current along about 18°N in HYCOM assimilation; (b) correlation between HYCOM result (Fig. 6c) and observations (Fig. 3) at 400-, 500-, and 600-m depths; and (c) as in Fig. 3, but for HYCOM assimilation.

eddies indicated in the figures of other months demonstrate the same relationship. Therefore, it can be inferred that the Kuroshio and the LUC are out of phase.

It is found from Fig. 5 that the currents at 313–689 m are closely related to the surface current V_s. The correlation coefficients between them are from 0.45 to 0.86 with confidence level above 99%. That indicates that the LUC ISV and the surface currents are highly related.

2) Results with NRL HYCOM assimilation

As there are few in situ field observations in the subsurface ocean, it is very difficult to display a full process of impact of surface or subthermocline eddies on the subsurface currents. Hereinafter, we present some facts of the interaction between mesoscale eddies and the LUC with HYCOM assimilation. Figure 6 illustrates some features of the LUC in the assimilation. Though the LUC core in HYCOM assimilation is relatively deeper than the observed, their values are nearly the same (Fig. 1b and Fig. 6a). Correlation between the assimilation and mooring data is statistically significant at 95% confidence level (Fig. 6b). On intraseasonal time scales, the LUC ISV in observations can be reproduced in the eddy-resolving HYCOM assimilation on both phases and periods except for segments 5a and 5b (Fig. 3 and Fig. 6c). As observed, ISVs at some depths in segments 3b and 5b propagate upward. Thus, in general HYCOM assimilation can be used for the LUC ISV analysis.

Time-averaged horizontal current anomalous field of each segment at 400-m depth is shown in Fig. 7. Obviously, mesoscale eddies at 400 m around the mooring site are significant and their patterns are similar with surface current in satellite data (Fig. 4). These westward-propagating eddies cross the mooring and might play a role in causing the LUC ISV.

3) What determines ISV vertical propagation direction and speed?

As mentioned above, the LUC ISV signal propagates vertically with certain speeds and directions in various segments. It is indicated through analysis that the LUC

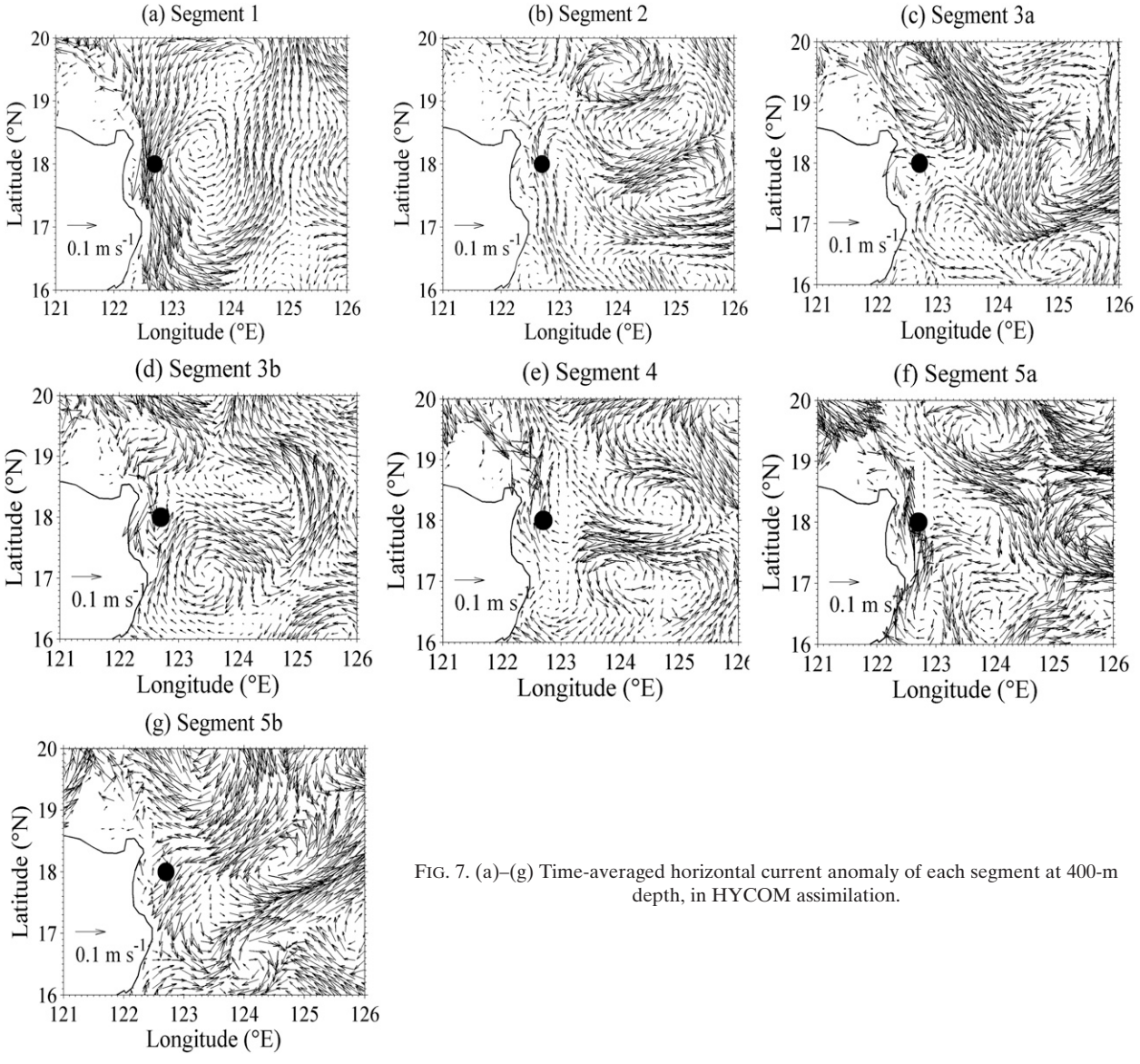

FIG. 7. (a)–(g) Time-averaged horizontal current anomaly of each segment at 400-m depth, in HYCOM assimilation.

ISV should result from the westward propagation of mesoscale eddies. Therefore, the effect of the zonal moving speed and vertical structure of these eddies is the real cause for the ISV vertical propagation direction and speed. Consequently, the key is how to determine the zonal speed of the eddy westward motion U and its vertical structure (slope of the eddy S), which, in what follows, are estimated with use of the NRL HYCOM assimilation.

1) To determine U: The westward-propagating speed of an eddy U can be roughly estimated by use of the satellite sea level anomaly, as shown in Table 1. For various segments, U values are within the range of 5–11 cm s^{-1} with an average of about 8 cm s^{-1}, which is very close to the 9.2 cm s^{-1} provided by Qiu and Chen (2010) for the subtropical countercurrent region (18°–25°N, 135°–170°E).
2) To determine S: The vertical structure of an eddy can be illustrated in a vertical section of its meridional velocity anomaly v'. To the subsurface ocean, v' between 300 and 700 m is shown in Fig. 8. A significant feature in Fig. 8 is that almost all the v' isolines are slanted. In the case of the slanted v' isolines, the horizontal westward movement of the eddy must induce a vertical phase propagation ISV at certain fixed point. Since the mesoscale eddies propagate westward and the radii of most eddies are larger than the distance between the mooring and coast (Fig. 4), the vertical phase propagation of LUC

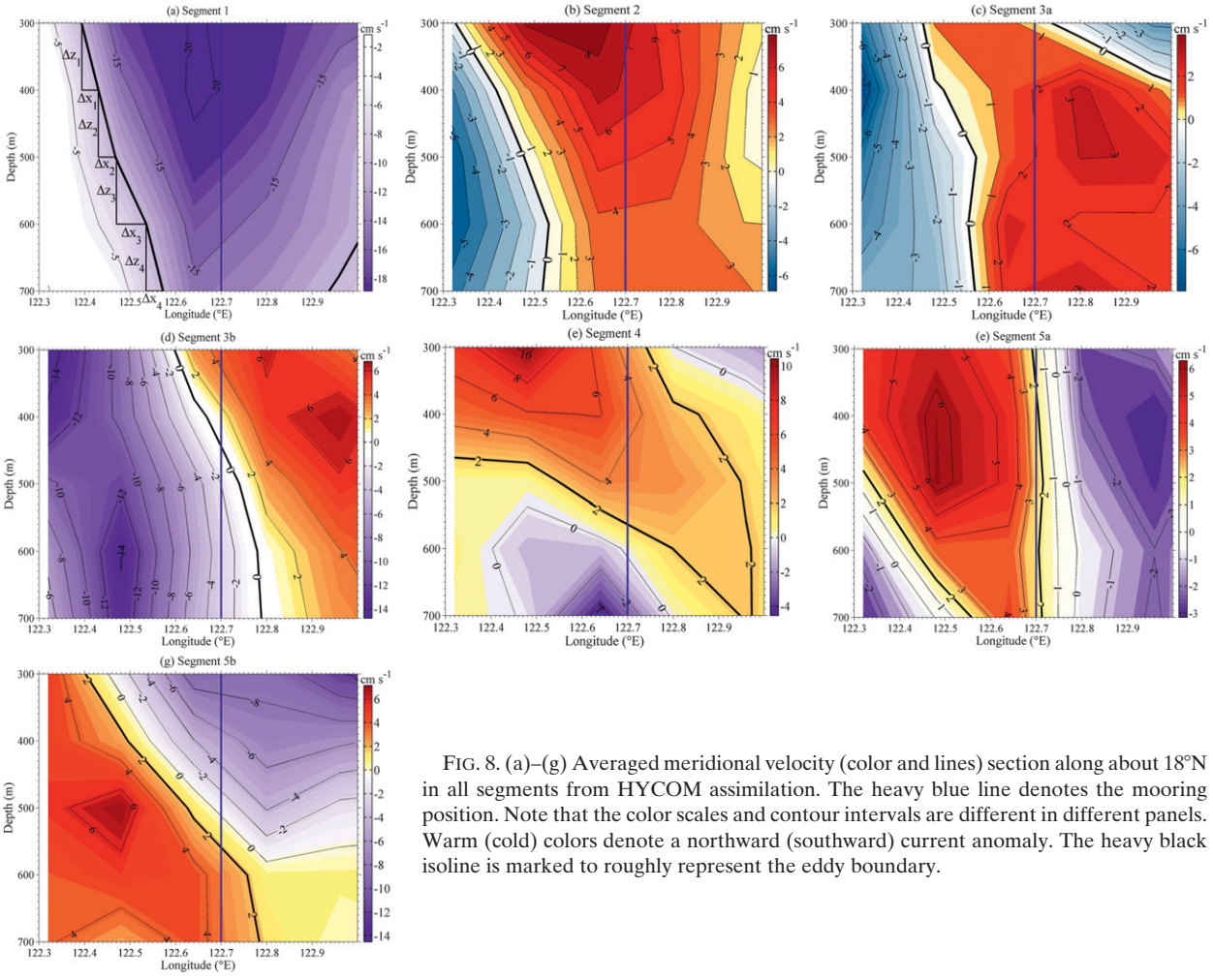

FIG. 8. (a)–(g) Averaged meridional velocity (color and lines) section along about 18°N in all segments from HYCOM assimilation. The heavy blue line denotes the mooring position. Note that the color scales and contour intervals are different in different panels. Warm (cold) colors denote a northward (southward) current anomaly. The heavy black isoline is marked to roughly represent the eddy boundary.

ISV results only from the slanted v' isolines to the left (by looking northward) of the eddy (Fig. 8). In what follows, we calculate the phase propagation with the slanted v' isoline to the left of the eddy with the HYCOM assimilation.

Then, the vertical phase propagation speed w_{eddy} can be calculated as follows:

$$w_{\text{eddy}} = US, \tag{1}$$

where $S = \Delta z_1/\Delta x_1$ and Δx_1 and Δz_1 are roughly determined by the heavy black v' isolines marked in Fig. 8a. As the vertical resolution of HYCOM assimilation is 100 m, the slope of the eddy (i.e., S) can be estimated every 100 m. Based on the zonal speed of eddy propagation (i.e., U; Table 1) and heavy black v' isolines (Fig. 8), w_{eddy} in each segment is estimated every 100 m and then the vertical average of w_{eddy} is easily calculated (Table 1).

It is found from Table 1 that the magnitudes of w_{eddy} and w_{ISV} are approximately of the same order except for the ones for 3b and 5b, which might be caused by poor HYCOM assimilation for subthermocline eddies.

In addition, the maximum ISV signal in segment 5b occurs at about 650-m depth, which is different from the other segments (Fig. 3). As suggested by Qu et al. (2012), the mesoscale fluctuations (50–100 days) in the subsurface ocean might be a result of subthermocline eddies that are mostly invisible at the sea surface. Unfortunately, the LUC ISV in segments 5a and 5b are poorly reproduced in HYCOM assimilation and so we could not make any definite conclusion up to now. Further investigation on subthermocline eddies off of Luzon Island and their role in LUC ISV is needed.

4. Summary and conclusions

The direct measurements of the LUC obtained for the first time are presented and some new characteristics of

the LUC are displayed. The maximum velocity of the LUC could exceed 27.5 cm s^{-1}, which is about four times stronger than the reported results in previous studies. The seasonality of the LUC from the direct measurements available at the mooring location is derived: LUC (winter) > LUC (summer) > LUC (spring). It is also found that the currents to the east of Luzon Island at 18°N, possess significant ISV from 70 to 80 days. From analysis of the satellite data and HYCOM assimilation, it is suggested that the westward movement of mesoscale eddies from the east might be the key for the LUC ISV. The westward-propagating speed and vertical structure of the westward-propagating eddy determine the phase speed and direction of the LUC ISV vertical propagation. In addition, the westward propagation of the eddy from the east causes the Kuroshio and the LUC to be out of phase on intraseasonal time scale.

Finally, it must be pointed out that the LUC disappeared and a northward flow took place in the whole observed column for about 50 days during the period from March to May. The cause of the event is still unknown. It may be due to either a shift of the LUC route from the mooring spot or a sudden event taking place during that period, which deserves further study.

Acknowledgments. The authors express their sincere gratitude to the crew of R/V *Science 1* as well as all scientists and technicians on board for the deployment or retrieval of the subsurface mooring to get these valuable data. The satellite dataset is provided by AVISO and the HYCOM assimilation is provided by Dr. Wei Cheng, and we are grateful to them. We express our hearty thanks to Dr. Bo Qiu for his very helpful discussion and suggestions. We are obliged to the two anonymous reviewers for their insightful and very helpful comments to the first manuscript. This study was supported by the National Key Basic Research Program of China (Program 973) (Grant 2013CB956202), the Major Project of National Natural Science Foundation of China (Grants 40890150 and 40890151) and the National Key Basic Research Program of China (Program 973) (Grant 2012CB417401).

REFERENCES

Chassignet, E. P., and Coauthors, 2009: US GODAE: Global ocean prediction with the Hybrid Coordinate Ocean Model (HYCOM). *Oceanography,* **22,** 64–75, doi:10.5670/oceanog.2009.39.

Dutrieux, P., 2009: Tropical western Pacific currents and the origin of intraseasonal variability below the thermocline. Ph.D. thesis, University of Hawaii at Manoa, 140 pp.

Firing, E., Y. Kashino, and P. Hacker, 2005: Energetic subthermocline currents observed east of Mindanao. *Deep-Sea Res. II,* **52,** 605–613, doi:10.1016/j.dsr2.2004.12.007.

Gao, S., T. Qu, and D. Hu, 2012: Origin and pathway of the Luzon Undercurrent identified by a simulated adjoint tracer. *J. Geophys. Res.,* **117,** C05011, doi:10.1029/2011JC007748.

Hu, D., and M. Cui, 1989: The western boundary current in the far-western Pacific Ocean, *Proc. Western Pacific Int. Meeting and Workshop on TOGA COARE,* Nouméa, New Caledonia, Centre Orstom de Nouméa, 123–134.

——, and ——, 1991: The western boundary current of the Pacific and its role in the climate. *Chin. J. Oceanol. Limnol.,* **9,** 1–14, doi:10.1007/BF02849784.

Kashino, Y., N. Espa, F. Syamsudin, K. J. Richards, T. Jensen, P. Dutrieux, and A. Ishida, 2009: Observations of the North Equatorial Current, Mindanao Current, and Kuroshio Current System during the 2006/07 El Niño and 2007/08 La Niña. *J. Oceanogr.,* **65,** 325–333, doi:10.1007/s10872-009-0030-z.

Kutsuwada, K., and H. Inaba, 1995: Year-long measurements of upper-ocean currents in the western equatorial Pacific by Acoustic Doppler Current Profilers. *J. Meteor. Soc. Japan,* **73** (2B), 665–675.

Qiu, B., and S. Chen, 2010: Interannual variability of the North Pacific subtropical countercurrent and its associated mesoscale eddy field. *J. Phys. Oceanogr.,* **40,** 213–225.

Qu, T., and R. Lukas, 2003: The bifurcation of the North Equatorial Current in the Pacific. *J. Phys. Oceanogr.,* **33,** 5–18.

——, T. Kagimoto, and T. Yamagata, 1997: A subsurface countercurrent along the east coast of Luzon. *Deep-Sea Res.,* **44,** 413–423, doi:10.1016/S0967-0637(96)00121-5.

——, H. Mitsudera, and T. Yamagata, 1998: On the western boundary currents in the Philippine Sea. *J. Geophys. Res.,* **103,** 7537–7548.

——, ——, and ——, 1999: A climatology of the circulation and water mass distribution near the Philippine Coast. *J. Phys. Oceanogr.,* **29,** 1488–1505.

——, T. L. Chiang, C. R. Wu, P. Dutrieux, and D. Hu, 2012: Mindanao Current/Undercurrent in an eddy-resolving GCM. *J. Geophys. Res.,* **117,** C06026, doi:10.1029/2011JC007838.

Roemmich, D., and J. Gilson, 2001: Eddy transport of heat and thermocline waters in the North Pacific: A key to interannual/decadal climate variability? *J. Phys. Oceanogr.,* **31,** 675–688.

Urick, R. J., 1983: *Principles of Underwater Sound*. McGraw-Hill, 384 pp.

Wang, Q., and D. Hu, 2012: Origin of the Luzon Undercurrent. *Bull. Mar. Sci.,* **88,** 51–60, doi:10.5343/bms.2011.1020.

Xie, L., J. Tian, D. Hu, and F. Wang, 2009: A quasi-synoptic interpretation of water mass distribution and circulation in the western North Pacific. II: Circulation. *Chin. J. Oceanol. Limnol.,* **27,** 955–965, doi:10.1007/s00343-009-9240-x.

Zhao, J., and D. H. Luo, 2010: Response of the Kuroshio Current to eddies in the Luzon Strait. *Atmos. Oceanic Sci. Lett.,* **3,** 160–164.

Zheng, Q., C. K. Tai, J. Hu, H. Lin, R. H. Zhang, F. C. Su, and X. Yang, 2011: Satellite altimeter observations of nonlinear Rossby eddy–Kuroshio interaction at the Luzon Strait. *J. Oceanogr.,* **67,** 365–376, doi:10.1007/s10872-011-0035-2.